Experimental Study on the Effect of the Spray Time on the Deflagration Characteristics of Oil Mist in a Closed Chamber

N. Zhou[1], Y. Zhang[1], X. Li[1†], B. Chen[2], Y. Wang[1], Z. Shi[1], M. Sun[1], C. Yang[3], X. Liu[4] and W. Huang[1]

[1] *School of Petroleum and Natural Gas Engineering, Changzhou University, Changzhou 213164, China*
[2] *Institute of Industrial Safety, China Academy of Safety Production Research, Beijing 100012, China*
[3] *School of Materials Engineering, Changshu Institute of Technology, Suzhou, 215500, China*
[4] *Tianjin Fire Research Institute of MEM, Tianjin 300381, China*

†*Corresponding Author Email: lix@cczu.edu.cn*

ABSTRACT

The deflagration of oil mist in closed chambers often causes severe ship fire accidents. Based on a self-built visual oil mist deflagration experiment platform, this research analyzed the effect of the spray time on the oil mist deflagration characteristics and focused on the flame propagation process, velocity, gas temperature, and overpressure in a closed chamber. The results show that with increasing spray time, the flame propagation velocity, gas temperature and deflagration overpressure increased. However, with the continuous increase in spray time, the deflagration characteristics of oil mist decreased. When the spray continued for 35 s, the peak overpressure was measured to be approximately 1.655 MPa. When the spray time extended to 95 s, the peak overpressure decreased by approximately 31.2% relative to the value at 35 s because the increase in spray time contributed to a more stable spray state and a larger diffusion range. Concurrently, the evaporation of liquid droplets increased of the kerosene vapor content. These factors contribute to a more intense oil mist deflagration. However, continuous increase in spray time results in an excessive accumulation of fuel, which makes an insufficient reaction and a significant reduction in deflagration characteristics. Oil mist deflagration process can be divided into four stages: deflagration, turbulent combustion, stretching and self-extinguishing. The high-temperature and high-pressure range of oil mist deflagration concentrate near the deflagration center, approximately 100 cm from left wall of the chamber.

1. INTRODUCTION

In the marine industry, spray fire poses a severe threat to the safety of ship and crew, and the engine room is where spray fire most frequently occurs. When the pipeline breaks, due to the high pressure in the pipeline, fuel will be sprayed into the air from the leakage port, and mist droplets will mix with air to form a fuel fog cloud. Once the ignition source is encountered, deflagration accidents may occur, damage the equipment in the engine room, make the ship lose power, and even cause secondary fire accidents, which results in ship destruction and death.

Kim et al. (2007) first performed gasoline spray deflagration experiments in an experimental platform of the simulated crew cabin of an armored vehicle with a volume of 3.78 m³. In the results, the spray deflagration temperature reached 102°C, the pressure reached 2.3 KPa,

and a longer spray time of 1–3 s corresponded to a greater deflagration pressure. Brophy et al. (1998) studied the detonation wave velocity and deflagration-to-detonation length of the JP-10/air mixture. The study showed that the ignition delay time was a key factor that determined the transformation from deflagration to detonation. Wang et al. (2017) conducted a deflagration experiment of fuel spray in a 3-m×3-m×3.4-m closed chamber. They found two types of spray deflagration: strong deflagration and weak deflagration, and the former had a higher overpressure than the latter. Strong deflagration produces a huge spherical flame in a very short time and subsequently quickly extinguishes. In contrast, the weak spray deflagration generated a longer-lasting spray flame.

Some scholars have discovered that the combustion of oil mist droplets is related to droplet parameters, nozzle structure, injection pressure and combustion Environment. Jinxian et al. (2008) experimentally investigated the

atmospheric pressure atomization combustion of gas/liquid coaxial nozzles and analyzed the effects of the nozzle structure and droplet parameters on the combustion performance. Hoover et al. (2005) revealed that when the diameter of droplets decreased at an unchanging equivalent proportion, the deflagration overpressure increased, and the flame velocity first increased and subsequently decreased. This behavior can be considered the transition of fuel spray from non-uniform combustion to uniform combustion (Chan & Jou, 1988; Chan & Wu, 1989; Hoover et al., 2005). Bai and Wang (2015) conducted spray explosion experiments with different concentrations of ether in a 20-L spherical container. The spray droplet size has a significant impact on the pressure, temperature and combustibility. Jia et al. (2023) conducted a deflagration experiment of inhomogeneous oil mist in a confined cabin and studied the effects of the nozzle size and nozzle pressure on the oil mist deflagration characteristics. They indicated that the increase in nozzle diameter and spray pressure both aggravated the deflagration strength of oil mist, and the nozzle size had a more significant effect on the deflagration intensity of oil mist than the spray pressure. Perdana et al. (2023) explored the combustion process of olive oil droplets under varying temperatures and magnetic field orientations. They discovered that the magnetic field could accelerate the combustion velocity and reduce ignition delay.

In addition, some scholars focused on the effect of the equivalence specific concentration on the oil mist deflagration characteristics. Parsinejad et al. (2006) studied the relationships between the equivalence ratio and the combustion rate, temperature and pressure. Bin and Xie conducted detonation performance experiments of various fuel clouds such as propylene oxide in vertical detonation tubes. They found a U-shaped relationship between critical initiation energy and equivalence ratio of the droplet cloud. The detonation velocity and explosion overpressure increased with increasing in equivalence ratio on the lean-burn side, whereas the detonation velocity tended to decrease with increasing equivalence ratio on the rich-burn side (Xie et al., 2003; Bin et al., 2010). Liu et al. (2016) found that the explosion temperature first increased and subsequently decreased with the increase in concentration. Liu et al. (2010) studied the deflagration to detonation process of nitromethane cloud with a concentration of 515 g/m^3 in a horizontal explosion tube and measured the pressure-time curve at this concentration, the peak overpressure and detonation velocity at different distances. Zabetakis (1964), Burgoyne et al. (1954) and Faeth and Olson (1968) found that under identical concentration conditions, the droplet diameter and distance between droplet affected the lower explosive limit of cloud. Danis et al. (1988) introduced the view that the gas phase concentration of liquid fuel would affect the lower explosive limit of cloud, but they did not quantify the gas phase concentration that corresponded to different volatile liquid fuels or analyze the effect of the gas phase concentration on the lower explosive limit of cloud. Benedick et al. (1991) discovered that detonation wave attenuation was faster in a gas-liquid two-phase system than in a gas-phase system; the attenuation rate of

detonation wave propagation was related to the properties of liquid fuel, including the viscosity, heat of evaporation, surface tension of the liquid droplet and amount of liquid per unit mass of gas. BarOr et al. (1981) conducted cloud detonation experiments on hydrocarbon fuels with different volatile properties. The results showed that the reaction zone of low-volatility fuel was long, the detonation wave velocity was lower than the theoretical CJ value of gas phase detonation, which was determined by the droplet breaking process, and the detonation wave velocity of high-volatility fuel was close to the theoretical CJ value of gas phase detonation. Kopyt et al. (1989) conducted a cloud detonation experiment in a large-volume (600 m^3) open space and recorded the flame propagation velocity of gasoline, kerosene, diesel and petroleum cloud detonation. Li and Zhou studied the influence of the ignition position on the oil mist deflagration characteristics. With the decrease in ignition distance, the deflagration intensified (Li et al., 2024; Zhou et al., 2024).

At present, the research on deflagration characteristics primarily focuses on flammable gases (such as methane and hydrogen), whereas the study of typical two-phase flow oil fog deflagration characteristics is relatively rare. The existing studies mainly concentrate on the spray combustion processes, fuel types, and continuous spray deflagration in vertical chambers. However, in scenarios such as oil pipeline ruptures and fuel leaks in engine rooms, the spray time directly affects the distribution and concentration of oil mist and significantly affects the deflagration intensity. To solve this problem, this study used similarity theory to design and construct an experimental platform to simulate oil mist deflagration in a horizontal cabin. The platform enabled the dynamic visualization of the entire oil mist deflagration process. This study investigated key parameters such as the flame propagation process, velocity, peak deflagration pressure, and temperature fields. It identified the optimal spray time that corresponded to the maximum deflagration intensity and revealed the staged characteristics of flame propagation, evolution patterns of the deflagration pressure and temperature distributions. These critical parameters provide foundational data support for the structural strength design of ship chambers, thermal protection design, and formulation of emergency response plans.

2. EXPERIMENTAL SETUP

The platform was composed of a chamber, a kerosene atomization system, an ignition system and a test system, as shown in Fig. 1(a). The chamber body was made of welded steel plates, and the front and rear sides of the chamber body were sealed with transparent acrylic plates, which were used as shooting windows. A high-speed camera was set in front of the center of the chamber, 3 m away from the front window. The kerosene atomization system consisted of a relief value, a pressure reducing valve, two solenoid valves, a check valve, a pressure gauge, a "U" type storage tube and a spray nozzle. The experiment used the pressure atomization method: Kerosene was pushed by high-pressure air to the nozzle
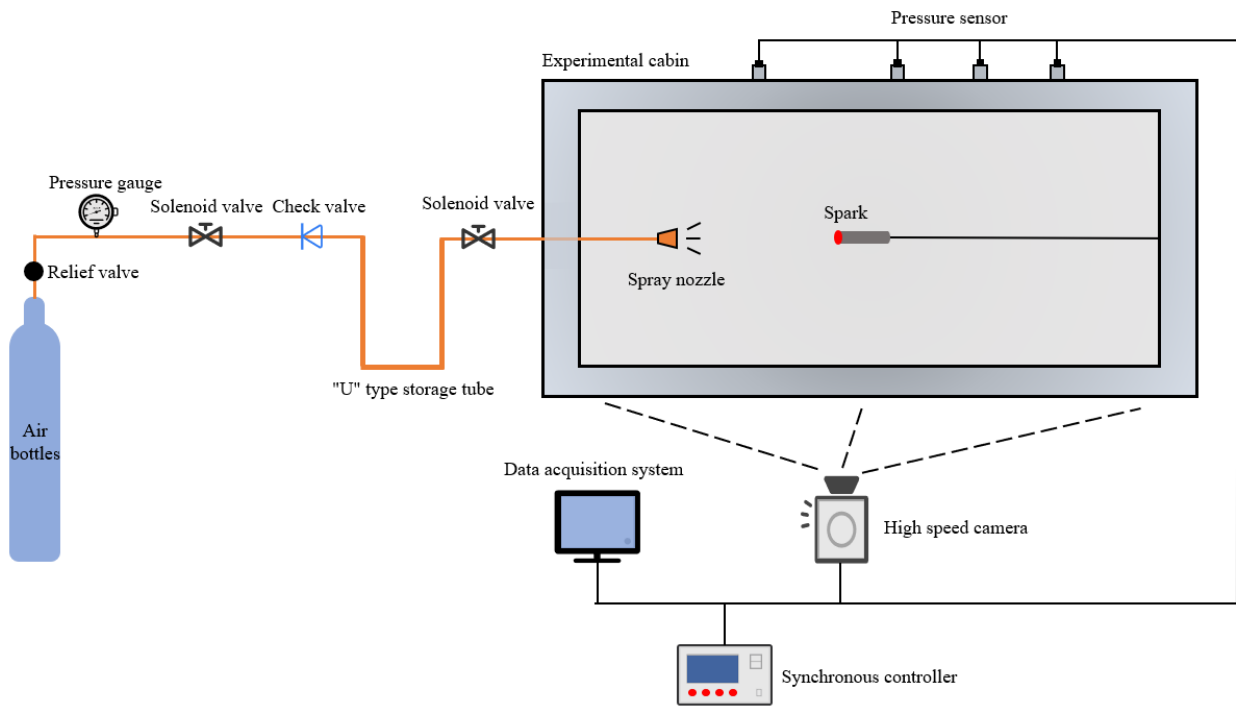
Fig. 1(a) Experimental system diagram
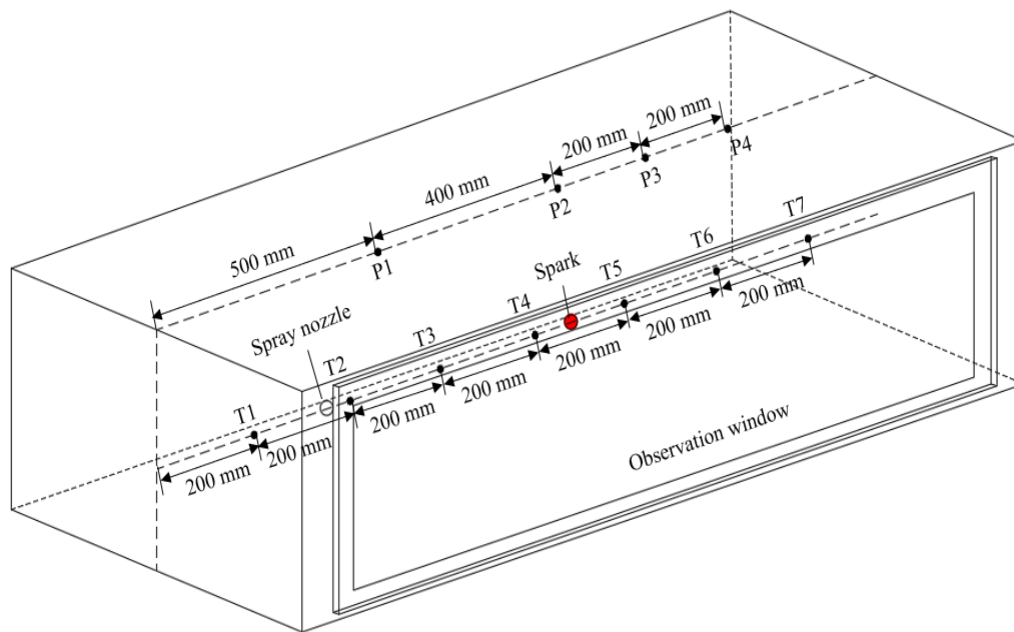
Fig. 1(b) Experimental chamber diagram (P1-P5: pressure sensors; T1-T7: temperature sensors)

and through the nozzle to form oil mist in the chamber. The pressure in the pipeline was regulated to 0.98 MPa by the relief valve. Under these experimental conditions, no oil mist was present in the initial environment, which resulted in an initial oil mist concentration of zero. We used nozzles with diameters of 0.1 mm, 0.3 mm, and 0.5 mm to investigate the deflagration characteristics of oil mist under different spray times. The findings indicate that an increase in nozzle size increased the oil mist concentration, and the deflagration characteristics of the oil mist intensified with longer spray times for these

nozzle sizes. Considering the length of the manuscript and the distinct variation trend exhibited by the 0.8-mm nozzle, i.e., the deflagration characteristics weakened with the increase in spray time, we selected the 0.8-mm nozzle case to conduct a detailed analysis.

The nozzle was mounted on the centerline of the chamber, which was approximately 380 mm from the left side wall; the ignition rod was installed 500 mm to the right of the nozzle. Figure 1(b) shows the specific location of the experimental measurement points and experimental

Table 1 Experimental Equipment Information

Equipment	Equipment parameter
I-speed camera	Pixel size 1280 * 1024, exposure time 1/8000 s, frame rate 200 fps
TST3406 dynamic testing analyzer	Acquisition rate 200k Hz, acquisition length 2000 k
EPT-6 ignition energy test platform	The ignition energy range is 100 mJ–19 J, and this experiment is set at 500 mJ with an ignition time of 5 ms
PCB 102B04 pressure sensor	Range 0.009–10 MPa, accuracy of ± 0.1% of full scale
WRNK-191K Flexible Thermocouple	Measurement range 0–1100°C, accuracy 0.1°C, response speed 10 ms

chamber. Table 1 shows the performance parameters of the ignition system and testing system. In this study, a high-speed camera was used to record the propagation of deflagration flames. By calculating the time required for the transient flame front to propagate to a certain location, the flame propagation velocity was quantitatively calculated (Wang et al., 2022).

The stability of the overall oil mist field in the experimental chamber, which is a closed space, includes the stability of the oil mist in the conical space sprayed by the nozzle and the stability of the oil mist field formed after the oil mist has diffused throughout the entire chamber. Although the oil mist in the conical space sprayed by the nozzle can be very quickly stabilized, the small amount of oil mist that diffuses to the surrounding area takes time (approximately 15 s) to stabilize. Therefore, we studied the effect of the spray time (5 s, 15 s, 35 s, 65 s, and 95 s) on the characteristics of ignited oil mist.

3. ERROR ANALYSIS

The uncertainty in experimental test results mainly arose from factors such as measurement methods, personnel, environmental fluctuations, and variations in the measured object. Based on the analysis of the research subject, we believe that the uncertainty in the experiments can be determined through statistical analysis methods. Therefore, we primarily use standard deviation analysis to evaluate the test errors. The standard deviation analysis is a statistical measure to quantify the degree of dispersion in numerical data. It represents the average deviation of a data point from the mean of the data set. During the testing process, the meteorological tester was used to record the environmental parameters. The temperature was maintained at 280–283.1 K, the relative humidity was 36–56%, and the wind speed was 0 m/s (indoor). To ensure the stability of the experiments, all test conditions were maintained consistent, and the experimental platform was placed in an indoor environment. The local environment inside the chamber had minimal impact on the tests, and the differences between repeated experiments were negligible. From a test design perspective, the construction of the experimental platform fully accounted for the precision of the equipment. The instruments in the test were of high accuracy to ensure that the instrument precision did not significantly affect the reliability of the experimental results. To enhance the reliability of the tests, each condition was repeated three times. Under identical test conditions, the error in the maximum overpressure was controlled to within 5%. After each test,

the exhaust system was activated to remove residual gases from the previous experiment. The kerosene residue at the bottom of the chamber was cleaned, and the chamber was allowed to return to ambient temperature before proceeding with the next test to ensure that no cross-contamination occurred between experimental groups.

4. RESULTS AND ANALYSIS

4.1 Flame Propagation Process Analysis

Figure 2 shows the oil mist deflagration process when the spray continued for 5 s. From the images, the deflagration process of oil mist is a complex multi-stage reaction and can be divided into four main stages: deflagration, turbulent combustion, stretching and self-extinguishing. In the deflagration stage, the oil mist is ignited by an electric spark and forms a small spherical flame at the ignition center. Due to the relative velocity between droplets and air, the flame transforms from a spherical shape to an elliptical shape and rapidly propagates throughout the entire spray region. Accompanied by a loud bang, the deflagration ends at approximately 180 ms. This stage is characterized by its short duration, where the flame instantaneously reaches its maximum length. The second phase is the turbulent combustion stage, where the turbulence environment triggered by the deflagration significantly impacts the flame propagation. The flame front curls due to the action of turbulent vortices and significantly increases the flame surface area. This turbulence-flame coupling enhances the mixing efficiency of fuel and oxygen and makes the flame pulsate at a certain frequency. When the combustion reaction proceeds, oxygen is rapidly consumed, and the incompletely combusted oil mist droplets generate a large amount of smoke due to incomplete thermal decomposition, which gradually decreases the flame brightness. The third phase is the stretching stage, where the shear and stretching effects of turbulent vortices make the airflow gradually diverge. Incompletely combusted droplets, under the condition of local oxygen depletion, further drove the flame front to stretch and expand toward areas with relatively higher oxygen concentrations. This asymmetric propagation causes significant fluctuations in flame shape and exhibits instability. The fourth stage is the self-extinguishing stage, during which the flame moves away from the spray area, wanders in the chamber, and exhibits the characteristic behavior of a wandering fire. As oxygen becomes depleted, the scattered flames are fully extinguished.

Deflagration stage

Turbulent combustion stage

Stretching stage

Self-extinguishing stage
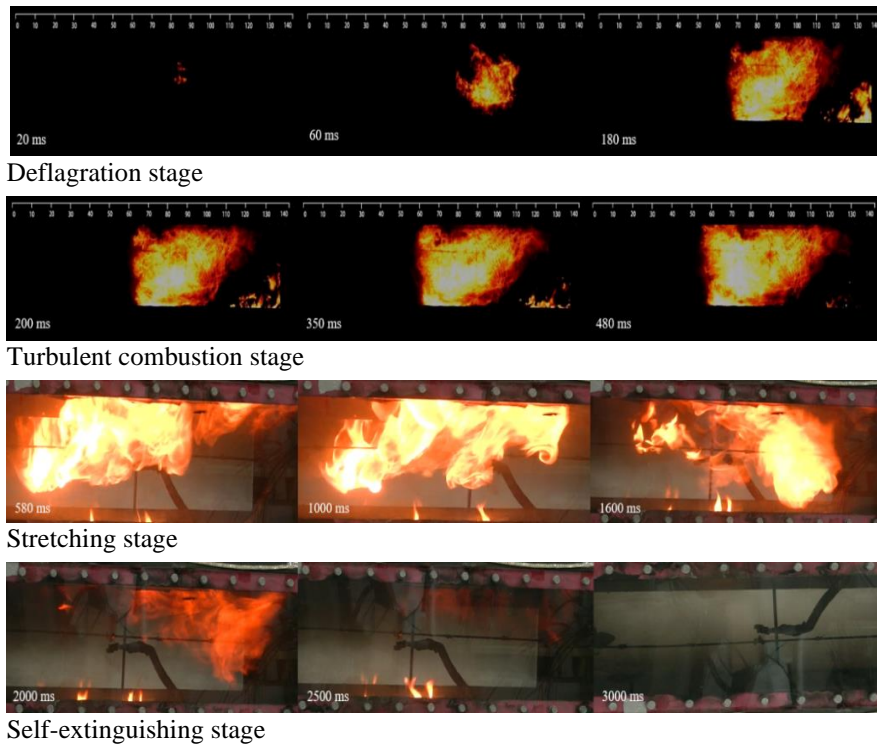
Fig 2 Oil mist deflagration process when the spray continues for 5 s

Figure 3 shows the flame images of the deflagration stage at different spray times. At the moment of ignition, kerosene produces high-temperature and high-pressure explosion products that continuously increase the temperature of the oil mist system. The light components of the oil mist rapidly vaporize to form combustible vapors, whereas the recombination component is thermal decomposition. Part of the recombination component is directly evaporated and enters the oxidation decomposition stage. Once the local ignition conditions are met, deflagration occurs. When the spray duration is short, the deflagration flame is relatively small and exhibits significant flame stretching. With a longer spray duration, more droplets settle and continuously evaporate, which increases the fuel concentration at the chamber floor. This increase leads to more intense deflagration in the lower half of the chamber and a larger flame area. Moreover, droplets that fail to evaporate in time accumulate at the bottom of the chamber to form a liquid pool, which ignites and causes a pool fire.

(a) Deflagration stage when the spray continues for 15 s

(b) Deflagration stage when the spray continues for 35 s

(c) Deflagration stage when the spray continues for 65 s

(d) Deflagration stage when the spray continues for 95 s
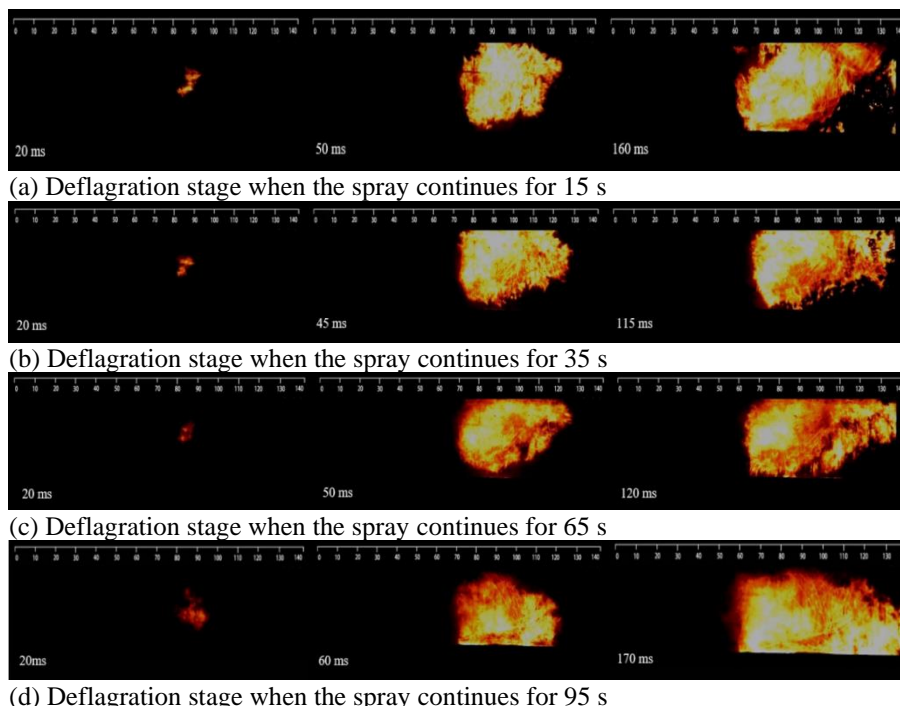
Fig. 3 Deflagration stage when the spray continues for different lengths of time
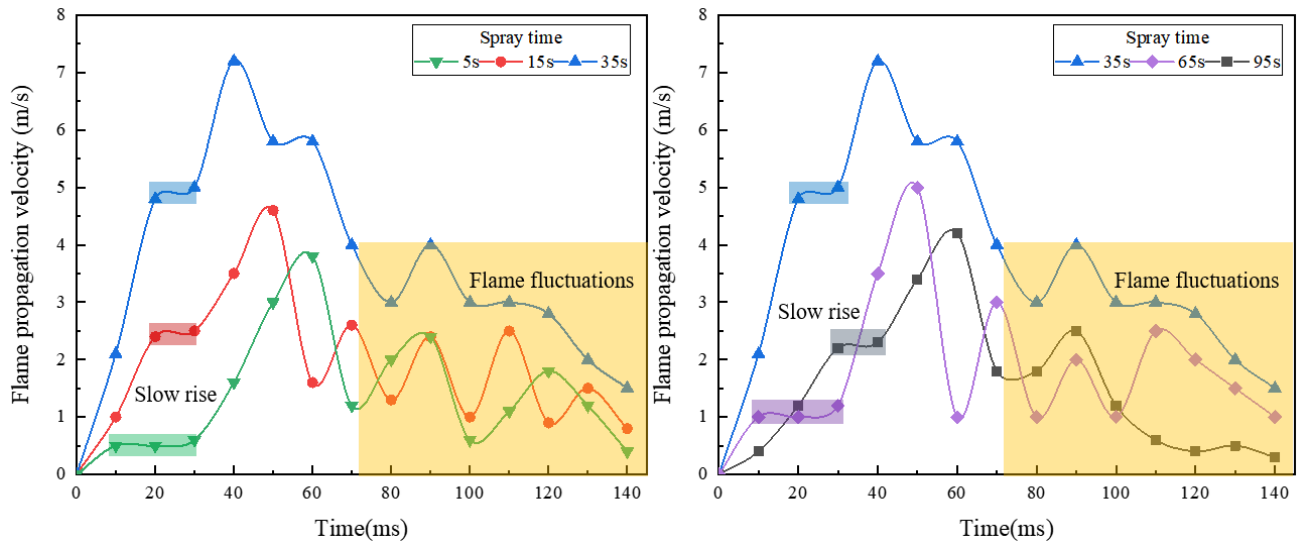
Fig. 4 Flame deflagration propagation velocity at different spray times
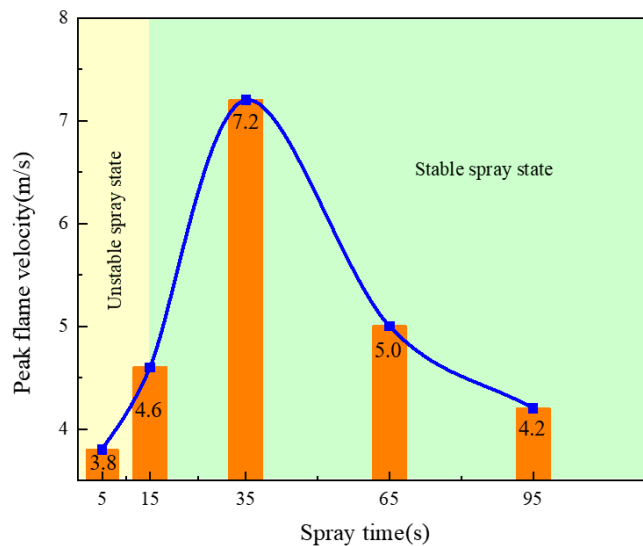
Fig. 5 Peak flame velocity at different spray times

4.2 Flame Velocity Analysis

Figure 4 exhibits the flame velocity during the deflagration stage for different spray time lengths. The flame propagation velocity in all conditions first increases, subsequently decreased, and oscillates with a peak velocity within 40–60 ms. When the spray continues for 35 s, the flame velocity reaches its peak value in the shortest amount of time. Prior to reaching the peak value, the flame velocity has a gradual increase because during the initial stage of deflagration, the ignition energy is utilized for the chain reaction of combustion and evaporation of liquid-phase fuel. When the oil mist is ignited, the flame becomes coupled with the pressure wave, increases the turbulence of the flow field, accelerates the turbulent combustion rate, and expedites the energy release. Consequently, the flame velocity rapidly increases. Furthermore, the roughness of the chamber walls and the heat dissipation and cooling effects cause significant momentum losses in the chamber (Barletta et al., 2007; Xu et al., 2023), which affects the

increase in flame propagation velocity. The high-temperature gas vaporizes the droplets, whereas the high-speed airflow deforms and breaks them. These processes of droplet fragmentation and evaporation accelerate the motion of the droplets and gas-phase particles, which leads to a sustained increase in flame velocity to the peak velocity. As the deflagration progresses, the flame velocity decreases because the reflection of the pressure wave upon reaching the right chamber wall intensifies the airflow perturbation in the chamber. The perturbation increases the flame instability, causes fluctuations in the flame propagation velocity, and promotes turbulence generation. The enhanced turbulence exerts a damping effect on the flame front and hinders its propagation in the chamber. Consequently, the curve illustrates a decrease in velocity.

As depicted in Fig. 5, the peak velocity under each condition appears to be relatively small. The reason is that the deflagration center is near the right side of the chamber, which makes the pressure wave quickly reach
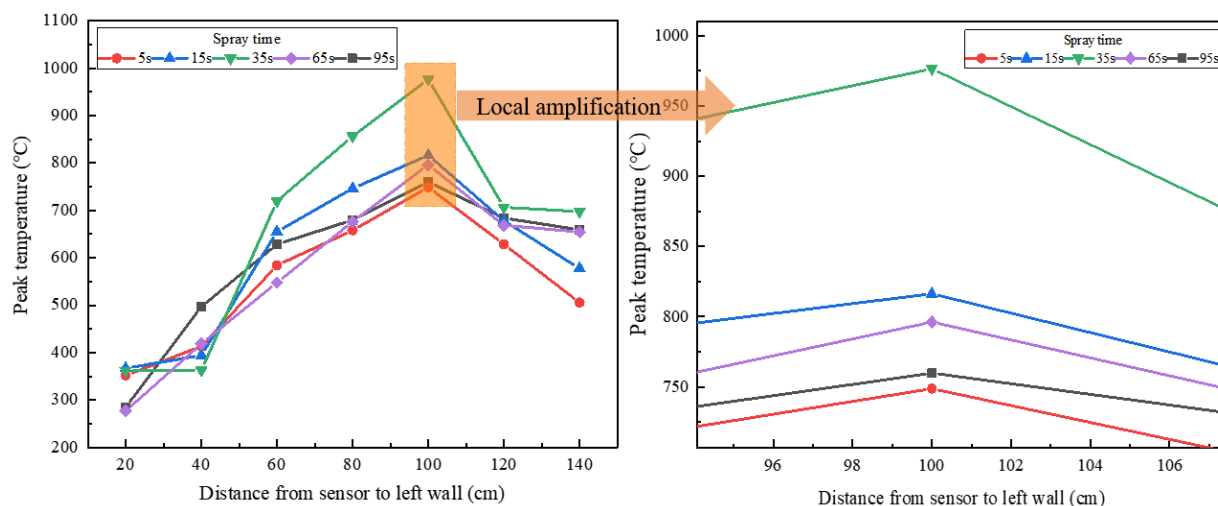
Fig. 6 Variation trend of the peak temperature at different spray times

the right wall, reflect, and hinder the development of the flame front. When the spray time is 0–5 s, the peak velocity first continues to increase. At 5 s, the peak velocity of flame propagation is the lowest (only 3.8 m/s). When the spray continues for 35 s, the peak velocity reaches 7.2 m/s, i.e., a 3.4-m/s increase, which is an 89.5% increase. However, when the spray time exceeds 35 s, the peak velocity decreases. At 95 s, the peak velocity is 4.2 m/s, which is a 3-m/s decrease compared to the value at 35 s, i.e., a 41.7% decrease. This trend can be explained by the instability of the kerosene spray at short spray times (less than 15 seconds), which makes it difficult to form a uniform spray. At the moment of deflagration, the heat exchange between the flame front and the droplets is insufficient to vaporize the larger droplets. The heat transfer among droplets absorbs heat, which decreases the flame propagation velocity. With longer spray time, the spray becomes more stable, and the droplets more densely diffuse and spread. The effective molecular collisions per unit time increase. Concurrently, when the droplets gradually evaporate and decrease in size, the kerosene vapor content in the chamber gradually increases (Ballal et al., 1975; Ballal & Lefebvre, 1981). These factors collectively lead to more intense deflagration and a higher peak velocity of flame propagation. When the spray time continues to increase, the excessively high concentration of oil mist leads to uneven mixing of fuel and oxygen in the turbulent field. This unevenness alters the structure of turbulence, causes small-scale vortices to be dissipated by high concentrations of vapor and droplets, which weakens the promoting effect of turbulence on flame propagation. Simultaneously, an excess of fuel vapor may increase the local heat capacity, reduce the efficiency of turbulent heat transfer, and consequently inhibit the velocity of flame propagation.

4.3 Gas Temperature Analysis

Figure 6 shows the effect of the spray time on gas temperature. As observed, the peak temperatures under various conditions are measured by the sensor at 100 cm. The peak temperatures first increase with the increase in spray time. When the spray continues for 5 s, the peak temperature is only 748.8°C. When the spray continues for

35 s, the peak temperature is 976.5°C, i.e., a 30.4% increase of 227.7°C. This increase is attributed to the deflagration center being located 100 cm from the left wall of the chamber, where the temperature is the highest. With the increase in spray time, the area of oil mist diffusion expands, and the average distance between droplets increases. The opportunity for oxygen molecules to contact the oil mist significantly increases, enhances deflagration and increases the peak temperatures. However, the peak temperature will also decrease with increased spray time. When the spray continues for 95 s, the peak temperature is 759.8°C, i.e., a 22.2% decrease of 216.7°C compared to the value at 35 s. The reason is that the changes in spray time directly affect the concentration of the oil mist. At a certain oil mist concentration, the density of droplets becomes too high, so adjacent droplets simultaneously compete for oxygen. The evaporation of the droplets absorbs heat, which decreases the temperature of the local area and consequently the overall peak average temperature. With the increase in concentration, this phenomenon becomes increasingly obvious (Liu et al., 2016). The temperature gradually decreases in the area far from the deflagration center. The theoretical combustion temperature of the fuel in this experiment is 1300°C. However, the experimental data value was slightly lower than the theoretical value due to the steel construction of the chamber, which has good thermal conductivity. Radiative loss to the surroundings and averaging effect of the thermocouple also decreased the temperature.

4.4 Deflagration Overpressure Analysis

Figure 7 illustrates the deflagration overpressure at different spray times. The peak overpressure first increased and subsequently decreased with longer spray time. When the spray was 35 s, the peak overpressure was 1.655 MPa, which is a 73.1% increase of 0.699 MPa compared to the value at 5 s. This increase is attributed to the gradual evaporation of droplets over time, which shrank them and enhanced the deflagration overpressure (Hoover et al., 2005). However, when the spray time exceeded 35 s, the peak overpressure significantly decreased with the increase in spray time. When the spray continued for 95 s, the peak overpressure was 1.138 MPa,
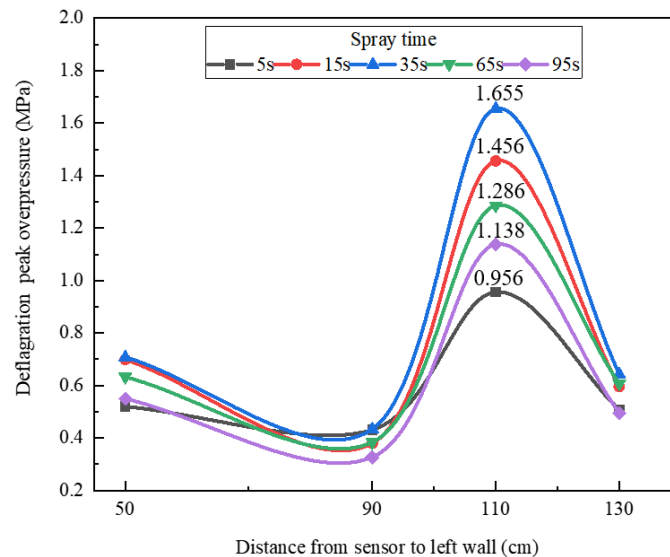
Fig. 7 Deflagration overpressure of oil mist at different spray times

which is a 31.2% decrease of 0.517 MPa compared to the value at 35 s. The reason is that an excess of kerosene vapor accumulated in the chamber, and the available oxygen was insufficient to support the reaction of this surplus fuel. Consequently, the reaction became extremely inadequate, which reduced the deflagration overpressure. In addition, the sensor at 50 cm from the left wall of the chamber recorded a higher pressure than the sensor near the ignition point at 90 cm because unburned droplets accumulated in this area, were affected by the pressure wave and left wall of the chamber, whose subsequent thermal expansion created a localized high-pressure zone (Ai et al., 2023). Combined with the flame propagation process, the flame mainly propagated to the right along the direction of the oil mist spray. The most intense deflagration occurred on the right side of the chamber, i.e., the location of the deflagration peak overpressure shifted rearward.

5. CONCLUSION

Based on a self-built visual oil mist deflagration experiment platform, this study investigated the effect of spray time on the oil mist deflagration characteristics in a closed chamber. The main conclusions are as follows:

(1) The oil mist deflagration process can be divided into four stages with significant differences: deflagration, combustion, stretching, and self-extinguishing. During the deflagration stage, the flame rapidly stretches from a spherical shape to an elliptical one and expands in a short duration. In the turbulent combustion stage, the flame curls due to the action of turbulent vortices and increases its surface area. In the stretching stage, the flame front extends toward areas with higher oxygen concentrations under the shear and stretch of turbulence, and the flame has a complex and unstable shape. In the self-extinguishing stage, the flame exhibits a wandering fire phenomenon and gradually vanishes.

(2) The increase in spray time does not always enhance the oil mist deflagration strength. With the

increase in spray time, the spray state tends to stabilize, and droplets disperse and decrease in size, which increases the deflagration intensity. However, an excessively high concentration of oil mist can weaken the promoting effect of turbulence on the flame propagation. When the spray continues for 95 s, the peak velocity is 4.2 m/s, i.e., a 41.7% decrease compared to the value at 35 s.

(3) In the deflagration center area (approximately 100 cm from the left chamber wall), the high temperature and high pressure are most concentrated: the maximum pressure is 1.655 MPa, and the highest temperature is 976.5°C. When the spray continues for 95 s, the peak overpressure decreases to 1.138 MPa, i.e., a 31.2% decrease compared to the value at 35 s.

(4) This study primarily investigated the deflagration characteristics of oil mist in a horizontal rectangular-shaped chamber. Research on the spray pressure and effects of the chamber size is currently not systematic, and the oil mist deflagration characteristics in chambers of other structural types have not been addressed. In future studies, the process and mechanism of oil mist deflagration in chambers of different volumes and structures can be analyzed, and a thorough foundational database can be constructed to offer support for the safety design and accident prevention of ship chambers.

CONFLICT OF INTEREST

The authors declare that there is no conflict of interest in this study.

AUTHORS CONTRIBUTION

Ning Zhou, reviewing and editing; **Yu Zhang**, writing-original draft preparation; **Xue Li**, reviewing and editing; **Bing Chen**: investigation; **Yun Wang**: experiment; **Zhuohan Shi**: data curation; **Mingxing Sun**: data curation; **Chunhai Yang**: investigation; **Xuanya Liu**: validation; **Weiqiu Huang**: validation.

REFERENCES

Ai, B., Gao, J., Hao, B., Guo, B., & Liang, J. J. J. o. A. F. M. (2023). Effect of obstacle length variation on hydrogen deflagration in a confined space based on large eddy simulations. *Journal of Applied Fluid Mechanics*, *17*(2), 384-397. https://doi.org/10.47176/jafm.17.02.2106

Bai, C., & Wang, Y. J. J. O. L. P. I. T. P. I. (2015). Study of the explosion parameters of vapor–liquid diethyl ether/air mixtures. *Journal of Loss Prevention in the Process Industries*, *38*, 139-147. https://doi.org/10.1016/j.jlp.2015.09.007

Ballal, D., Lefebvre, A. J. C., & Flame. (1975). The influence of spark discharge characteristics on minimum ignition energy in flowing gases. *Combustion and Flame*, *24*, 99-108. https://doi.org/10.1016/0010-2180(75)90132-7

Ballal, D. R., & Lefebvre, A. H. (1981). *Flame propagation in heterogeneous mixtures of fuel droplets, fuel vapor and air.* Symposium (International) on combustion. https://doi.org/10.1016/S0082-0784(81)80037-9

Bar-Or, R., Sichel, M., & Nicholls, J. (1981). *The propagation of cylindrical detonations in monodisperse sprays.* Symposium (International) on Combustion. https://doi.org/10.1016/S0082-0784(81)80163-4

Barletta, A., Magyari, E. J. I. J. o. H., & Transfer, M. (2007). Forced convection with viscous dissipation in the thermal entrance region of a circular duct with prescribed wall heat flux. *International Journal of Heat and Mass Transfer,* 50(1-2), 26-35. https://doi.org/10.1016/j.ijheatmasstransfer.2006.06.036

Benedick, W. B., Tieszen, S. R., Knystautas, R., & Lee, J. H. S. (1991). Detonation of unconfined large-scale fuel spray-air clouds. *Progress in Astronautics and Aeronautics*, *133*, 297-310. https://doi.org/10.2514/5.9781600866067.0297.0310

Bin, L. I., Li-Feng, X., Ou-Qi, N. I., Li-Fang, R., & Zheng-Hong, W. J. J. O. B. (2010). Study on detonation characteristics of fuel drops cloud. *Dandao Xuebao (Journal of Ballistics)*, *22*(2), 90-93. https://api.semanticscholar.org/CorpusID:102319845

Brophy, C. M., Netzer, D. W., & Forster, D. L. (1998). *Detonation studies of JP-10 with oxygen and air for pulse detonation engine development.* 34th AIAA/ASME/SAE/ASEE Joint Propulsion Conference and Exhibit. https://doi.org/10.2514/6.1998-4003

Burgoyne, J., Cohen, L. J. P. O. T. R. S. O. L. S. A. M., & Sciences, P. (1954). The effect of drop size on flame propagation in liquid aerosols. *Proceedings of the Royal Society of London. Series A. Mathematical and Physical Sciences*, *225*(1162), 375-392. https://doi.org/10.1098/rspa.1954.0210

Chan, K. K., & Jou, C. S. J. F. (1988). An experimental and theoretical investigation of the transition phenomenon in fuel spray deflagration: 1. The experiment. *Fuel*, *67*(9), 1223-1227. https://doi.org/10.1016/0016-2361(88)90042-7

Chan, K. K., & Wu, S. R. J. F. (1989). An experimental and theoretical investigation of the transition phenomenon in fuel spray deflagration: 2. The model. *Fuel*, *68*(2), 139-144. https://doi.org/10.1016/0016-2361(89)90313-X

Danis, A. M., Namer, I., Cernansky, N. P. J. C., & flame. (1988). Droplet size and equivalence ratio effects on spark ignition of monodisperse N-heptane and methanol sprays. *Combustion and Flame*, *74*(3), 285-294. https://doi.org/10.1016/0010-2180(88)90074-0

Faeth, G. M., & Olson, D. R. J. S. T. (1968). The ignition of hydrocarbon fuel droplets in air. *SAE Transactions*, 1793-1802. https://doi.org/10.4271/680465

Hoover, J., Bailey, J., Willauer, H., & Williams, F. J. N. M. R. (2005). Evaluation of submarine hydraulic system explosion and fire hazards. *NRL Memorandum Report*, 6180-6105. https://api.semanticscholar.org/CorpusID:107992601

Jia, J., Yao, G., Li, Q., Xu, J., & Lu, S. J. C. S. i. T. E. (2023). Experimental study on deflagration characteristics of non-uniform oil mist in an enclosed chamber. *Case Studies in Thermal Engineering*, *51*, 103586. https://doi.org/10.1016/j.csite.2023.103586

Jinxian, L., Haobo, H., & Chunguo, Y. J. J. O. A. (2008). Experimental research on gas/liquid coaxial swirling nozzle of atomization and combustion under normal pressure. *Journal of Astronautics*, *29*(5), 1563-1569. https://www.researchgate.net/publication/296761541_Experimental_research_on_gasliquid_coaxial_swirling_nozzle_of_atomization_and_combustion_under_normal_pressure

Kim, A., Liu, Z., & Crampton, G. (2007). Study of Explosion Protection in a Small Compartment. *Fire Technology*, *43*(2), 145-172. https://doi.org/10.1007/s10694-007-0008-6

Kopyt, N. K., Struchaev, A. I., Krasnoshchekov, Y. I., Rogov, N. K., Shamshev, K. N. J. C., Explosion, & Waves, S. (1989). Combustion of large volumes of dispersed fuels and the evolution of their products in the free atmosphere. *Combustion, Explosion and Shock Waves*, *25*(3), 279-285. https://doi.org/10.1007/BF00788797

Li, Q., Jia, J., Lin, J., Xu, J., & Lu, S. J. I. J. o. T. S. (2024). Effect of ignition distance on deflagration characteristics of non-uniform oil mist in closed cabins. *International Journal of Thermal Sciences*, *198*, 108887. https://doi.org/10.1016/j.ijthermalsci.2024.108887

Liu, Q., Bai, C., Jiang, L., Dai, W. J. C., & flame. (2010). Deflagration-to-detonation transition in nitromethane mist/aluminum dust/air mixtures. *Combustion and Flame*, *157*(1), 106-117. https://doi.org/10.1016/j.combustflame.2009.06.026

Liu, X., Wang, Y., & Zhang, Q. J. F. (2016). A study of the explosion parameters of vapor–liquid two-phase JP-10/air mixtures. *Fuel*, *165*, 279-288. https://doi.org/10.1016/j.fuel.2015.10.081

Parsinejad, F., Arcari, C., Metghalchi, H. J. C. S., & Technology. (2006). Flame structure and burning speed of JP-10 air mixtures. *Combustion Science and Technology*, *178*(5), 975-1000. https://doi.org/10.1080/00102200500270080

Perdana, D., Hanifudin, M., Rosidin, M., & Winarko, W. J. J. O. A. F. M. (2023). Characteristics of olive oil droplet combustion with various temperatures and directions of magnetic fields in the combustion chamber. *Journal of Applied Fluid Mechanics*, *16*(9), 1828-1838. https://doi.org/10.47176/jafm.16.09.1735

Wang, C., Liu, H., Yang, S., Guo, F., Sun, H., & Liu, X. (2017). Experimental study of spray deflagration mode in an enclosed compartment. *Journal of Loss Prevention in the Process Industries*, *50*, 1-6. https://doi.org/10.1016/j.jlp.2017.08.013

Wang, T., Yang, P., Yi, W., Luo, Z., Cheng, F., Ding, X., & Protection, E. (2022). Effect of obstacle shape on the deflagration characteristics of premixed LPG-air mixtures in a closed tube. *Process Safety and Environmental Protection,* 168, 248-256. https://doi.org/10.1016/j.psep.2022.09.079

Xie, L. F., Guo, X. Y., Guo, H. J. E., & Waves, S. (2003). Experimental study on the direct initiation of detonation in fuel-air sprays. *Explosion and Shock Waves*, *23*(1), 78-80. https://kns.cnki.net/kcms2/article/abstract?v=HgkNO Cd8VPiBPYnrXEsPmi89mGkvqQHCRwV6vMeviu PgMezef4se8GVM9pU2P96-Th0S5j2MZs6H-AoyS7wpVHjXMzaQJXooY_MRj6e5tBtr-BLfZ0ezF2P6eL7nFzuh14WXmvkEVicxDSqy0hkZ YDyFan9jeweI&uniplatform=NZKPT

Xu, A., Xu, B. R., & Xi, H. D. J. J. O. F. M. (2023). Wall-sheared thermal convection: heat transfer enhancement and turbulence relaminarization. *Journal of Fluid Mechanics,* 960, A2. https://doi.org/10.1017/jfm.2023.173

Zabetakis, M. G. (1964). *Flammability characteristics of combustible gases and vapors.* Bureau of Mines, Pittsburgh, PA. United States, Issue. https://doi.org/10.2172/7328370

Zhou, N., Wang, Y., Li, X., Yin, Q., Shi, Z., Zhao, P., & Effects, E. (2024). Study on the influence of ignition position on the deflagration characteristics of oil mist in ship cabins. *Energy Sources, Part A: Recovery, Utilization, and Environmental Effects*, *46*(1), 450-461. https://doi.org/10.1080/15567036.2023.2284995